Gas-Phase Oxidation Reactions of Ta2+: Synthesis and Properties of TaO2+ and TaO22+

ARTICLE *in* THE JOURNAL OF PHYSICAL CHEMISTRY A · MARCH 2012

Impact Factor: 2.69 · DOI: 10.1021/jp300294c · Source: PubMed

6 AUTHORS, INCLUDING:

Célia Lourenço
The Open University (UK)
6 PUBLICATIONS **16** CITATIONS
SEE PROFILE

Maria Conceição Oliveira
Technical University of Lisbon
37 PUBLICATIONS **304** CITATIONS
SEE PROFILE

THE JOURNAL OF PHYSICAL CHEMISTRY A

Article

pubs.acs.org/JPCA

Gas-Phase Oxidation Reactions of Ta^{2+}: Synthesis and Properties of TaO^{2+} and TaO_2^{2+}

Marta Santos,[†] Maria del Carmen Michelini,[‡] Célia Lourenço,[§] Joaquim Marçalo,[†] John K. Gibson,[∥] and Maria Conceição Oliveira*[,§]

[†]Unidade de Ciências Químicas e Radiofarmacêuticas, Instituto Tecnológico e Nuclear, 2686-953 Sacavém, Portugal

[‡]Dipartimento di Chimica, Università della Calabria, 87030 Arcavacata di Rende, Italy

[§]Centro de Química Estrutural, Instituto Superior Técnico, Universidade Técnica de Lisboa, 1049-001 Lisboa, Portugal

[∥]Chemical Sciences Division, Lawrence Berkeley National Laboratory, Berkeley, California 94720, United States

ABSTRACT: Gas-phase reactions of Ta^{2+} and TaO^{2+} with oxidants, including thermodynamically facile O-atom donor N_2O and ineffective donor CO, as well as intermediate donors C_2H_4O (ethylene oxide), H_2O, O_2, CO_2, NO, and CH_2O, were studied by Fourier transform ion cyclotron resonance mass spectrometry. All oxidants reacted with Ta^{2+} by electron transfer yielding Ta^+, in accord with the high second ionization energy of Ta (ca. 16 eV). TaO^{2+} was also produced with N_2O, H_2O, O_2, and CO_2, oxidants with ionization energies above 12 eV; CO reacted only by electron transfer. The following charge separation products were also observed: TaN^+ and TaO^+ with N_2O; and TaO^+ with O_2, CO_2, and CH_2O. $TaOH^{2+}$, formed with H_2O, reacted with a second H_2O by proton transfer. TaO^{2+} abstracted an electron from N_2O, H_2O, O_2, CO_2, and CO. Oxidation of TaO^{2+} by N_2O was also observed to produce TaO_2^{2+}; on the basis of density functional theory (DFT) results, this species is a dioxide, $\{O-Ta-O\}^{2+}$. TaO_2^{2+} reacted by electron transfer with N_2O, CO_2, and CO to give TaO_2^+. Additionally, it was found that TaO_2^{2+} oxidizes CO to CO_2 and that it acts as a catalyst in the oxidation of CO by N_2O. TaO_2^{2+} also activates H_2 to form TaO_2H^{2+}. On the basis of the rates of electron transfer from N_2O, CO_2, and CO to Ta^{2+}, TaO^{2+}, and TaO_2^{2+}, the following estimates were made for the second ionization energies of Ta, TaO, and TaO_2: $IE[Ta^+] = 15.8 \pm 0.3$ eV, $IE[TaO^+] = 16.0 \pm 0.5$ eV, and $IE[TaO_2^+] = 16.9 \pm 0.4$ eV. These IEs, together with recently reported bond dissociation energies, $D[Ta^+-O]$ and $D[OTa^+-O]$, result in the following bond energies: $D[Ta^{2+}-O] = 657 \pm 58$ kJ mol^{-1} and $D[OTa^{2+}-O] = 500 \pm 63$ kJ mol^{-1}, the first of which is in good agreement with the value obtained by DFT.

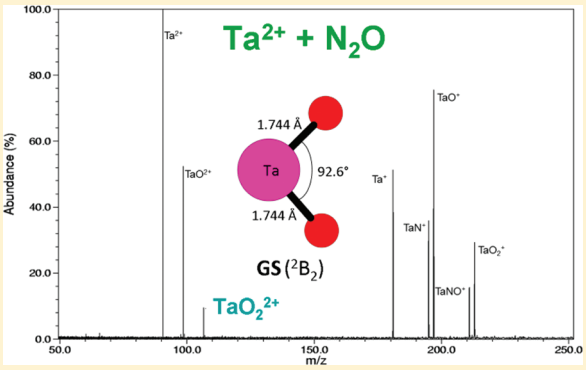

INTRODUCTION

Transition-metal oxides play important roles in many branches of chemistry. To fully understand their properties, the study of the energetics of elementary species in the gas phase is necessary. The gas-phase thermochemistry of tantalum oxides is not fully established. Only recently have the bond dissociation energies of TaO^+ and TaO_2^+ been reliably determined by Armentrout and co-workers as $D_0[Ta^+-O] = 676 \pm 12$ kJ mol^{-1}[1,2] and $D_0[OTa^+-O] = 587 \pm 12$ kJ mol^{-1}.[2] These authors analyzed the nature of the bonding in these species using the B3LYP/HW+/6-311+G(3df) level of theory; bond dissociation energies obtained using this and other levels of theory were in reasonable agreement with the experimentally determined values.[1,2] For the doubly charged Ta monoxide and dioxide, there are no corresponding thermodynamic values available, as there are no reports of gas-phase studies of the oxidation of Ta^{2+} cations. The reactivity of Ta^{2+} with alkanes was studied by Freiser and co-workers some twenty years ago,[3] and Armentrout and co-workers have recently reexamined the reaction of Ta^{2+} with methane.[4] Gas-phase reactions of Ta^+ ions with several oxidants, namely, O_2,[5] N_2O,[6] NO,[7] CO_2,[8] and D_2O,[9] have been studied by Bohme and co-workers during the past decade. Several matrix isolation infrared spectroscopic studies of the reactions of Ta metal and Ta oxides with oxidants have also been performed during the past decade.[10−15]

We have previously used Fourier transform ion cyclotron resonance mass spectrometry (FTICR/MS) to study the gas-phase oxidation reactions of several doubly charged actinide and lanthanide cations,[16−19] experiments that provided estimates of the ionization energies and bond dissociation energies of monoxides and dioxides. The same methods were used in studies of the reactivity of doubly charged actinide and lanthanide cations with hydrocarbons.[20−23] In the present work, we use a similar approach to examine the gas-phase

Received: January 10, 2012
Revised: March 7, 2012
Published: March 12, 2012

Table 1. Reactions of Ta^{2+}[a]

	N_2O	C_2H_4O	H_2O	O_2	CO_2	NO	CH_2O	CO
Ta^{2+}	0.41 [0.59]	0.35 [1.22]	0.27 [1.19]	0.47 [0.53]	0.48 [0.65]	0.38 [0.48]	0.23 [1.04]	0.025 [0.035]
	TaO^{2+}/35%	Ta^+/100%	TaO^{2+}/10%	TaO^{2+}/25%	TaO^{2+}/70%	Ta^+/100%	Ta^+/75%	Ta^+/100%
	Ta^+/30%		$TaOH^{2+}$/25%	Ta^+/65%	Ta^+/10%		TaO^+/25%	
	TaN^+/20%		Ta^+/65%	TaO^+/10%	TaO^+/20%			
	TaO^+/15%							

[a]The reaction efficiencies, k/k_{COL}, are given; the values in brackets are the pseudofirst-order reaction rate constants, k, in units of 10^{-9} cm^3 $molecule^{-1}$ s^{-1}. The absolute values are considered accurate to ±50%; the relative values for comparative purposes are considered accurate to ±20%.

Table 2. Thermodynamics of Oxidants, XO[a]

XO	N_2O	C_2H_4O	H_2O	O_2	CO_2	NO	CH_2O	CO
D[X−O] (kJ mol^{-1})	167	354	491	498	532	631	751	1076
IE[XO] (eV)	12.89	10.56	12.62	12.07	13.78	9.26	10.88	14.01

[a]From ref 40. The bond energies (D[X−O]) are accurate to 1 kJ mol^{-1} or less; the ionization energies (IE[XO]) are accurate to 0.01 eV or less.

reactivity of Ta^{2+} with oxidants. Density functional theory (DFT) computations were performed to evaluate the structures, bonding, and energetics of TaO^{2+} and TaO_2^{2+}.

EXPERIMENTAL DETAILS

The experimental procedures have been previously described,[16−23] and only a summary is presented here. The experiments were performed with an Extrel-Finnigan FT/MS 2001- DT 3-Tesla FTICR mass spectrometer, controlled by a Finnigan Venus Odyssey data system. Doubly charged tantalum cations were produced by laser desorption/ionization using a Spectra-Physics Quanta-Ray GCR-11 Nd:YAG laser operated at the fundamental wavelength (1064 nm). The reagent gases (N_2O, O_2, CO_2, NO, CO, and H_2) were all commercial products (>99% purity) and used as supplied. Dry, gaseous CH_2O was prepared by thermal decomposition under vacuum of (commercial) paraformaldehyde. C_2H_4O (>99% ethylene oxide) was degassed prior to its use. H_2O was thoroughly deoxygenated with N_2 and then degassed by multiple freeze−evacuation−thaw cycles. The neutral reagents were introduced into the mass spectrometer through leak valves to pressures in the range of 5×10^{-8} to 5×10^{-7} Torr and their purities confirmed from electron ionization mass spectra. The pressures were measured with a Bayard-Alpert type ionization gauge calibrated using standard reactions and corrected for the relative sensitivities of the gases. Isolation of the Ta^{2+} ions was achieved using single-frequency, frequency-sweep, or SWIFT excitation.[24]

The tantalum oxide and hydroxide ions, TaO^{2+}, TaO_2^{2+}, or $TaOH^{2+}$, when formed in sufficient amounts with a particular reagent, were also isolated using the same techniques. In some cases, the Ta oxide ions were produced by reaction of the Ta^{2+} with N_2O introduced into the spectrometer through pulsed valves, to study their subsequent reactions with other reagents. The reactant ions were thermalized by collisions with argon introduced into the spectrometer through pulsed valves to pressures of ca. 10^{-5} Torr or through a leak valve to pressures in the range of $(1−5) \times 10^{-6}$ Torr; electron transfer from Ar to the reactant ions was not observed. The reproducibility of the product distributions and reaction kinetics for different collisional cooling periods and/or collision gas pressures, as well as the linearity of the kinetics plots, indicated the thermalization of the reactant ions. Rate constants, k, were determined from the pseudofirst-order decay of the relative signals of the reactant ions as a function of time at constant neutral pressures. Reaction efficiencies, k/k_{COL}, were obtained using the collisional rate constants, k_{COL}, from the theory of Su and Chesnavich,[25] calculated using experimental molecular polarizabilities and dipole moments of the neutral reagents.[26] The main source of uncertainty in the absolute rate constants is the pressure measurement, and errors of ±50% are assigned to them; relative rate constants for different reactions are estimated to be accurate to ±20%, while typical precisions for replicate measurements of the same reaction are ±10%. The background in the spectrometer mainly consisted of water and air, with base pressures of $(1−2) \times 10^{-8}$ Torr, that is, ca. an order of magnitude lower than the reagent pressures used. Nevertheless, care was taken to minimize the interference of residual water and oxygen in the oxidation reactions and all the reactions were compared with those occurring under background conditions.

COMPUTATIONAL DETAILS

Quantum chemical computations were performed within the framework of DFT using the B3LYP[27,28] hybrid functional. The Stuttgart "SDD" small-core (60 core electrons) scalar relativistic effective core pseudopotentials (RECPs) and associated valence basis sets[29,30] were used for Ta while all-electron polarized valence triple-ζ DFT orbital basis sets (TZVP)[31] were used for O atoms. Geometry optimizations were performed without symmetry restrictions. Analytical frequencies were calculated in order to confirm that the optimized structures are local minima on the potential energy surface of the system and to evaluate the zero-point vibrational energy (ZPVE) corrections to the electronic energies, which are included in all the reported energies. Ultrafine pruned grids for numerical integration were employed in all the computations. Calculations were performed using spin-unrestricted methods. Different spin multiplicities were tested in order to establish the ground spin state. In particular, doublet and quartet spin states were considered for TaO^{2+}, and doublet, quartet, and sextet for TaO_2^{2+}. In both cases, the doublet spin state was found to be the ground spin state. All calculations were carried out with Gaussian09 package.[32]

The Natural Population Analysis (NPA)[33] and Atoms in Molecules (AIM)[34] approaches were used to determine the atomic charge distributions. Bonding analyses were performed using NBO (Natural Bond Orbital),[33] ELF (Electron Localization Function),[35,36] and AIM methodologies. The Top-

dx.doi.org/10.1021/jp300294c | J. Phys. Chem. A 2012, 116, 3534−3540

Mod[37,38] and AIMAll[39] packages were used to perform the ELF and AIM analyses.

RESULTS AND DISCUSSION

Reactions of Ta^{2+} with Oxidants: Formation of TaO^{2+}. The results obtained for the reactions of Ta^{2+} with oxidants, N_2O, C_2H_4O (ethylene oxide), H_2O, O_2, CO_2, NO, CH_2O, and CO, are presented in Table 1. In Table 2, we present pertinent thermodynamic data for the oxidants. The second ionization energy of Ta, IE[Ta^+] = 16.2 ± 0.5 eV,[41] exceeds the first ionization energies of each of the oxidants by at least 2 eV (see Table 2), and therefore, electron transfer from the neutral oxidants to give Ta^+ was an observed pathway with each oxidant. Charge separation channels were observed with N_2O, with the formation of TaN^+ and TaO^+, and with O_2, CO_2, and CH_2O, with the formation of TaO^+. TaO^{2+} was produced with N_2O, H_2O, O_2, and CO_2 oxidants with ionization energies above 12 eV (see Table 2). CO, with an ionization energy of 14 eV but an extremely high C−O dissociation energy (see Table 2), reacted only by electron transfer. $TaOH^{2+}$ was also formed with H_2O; this product may either comprise a hydroxide, Ta^{2+}−OH, which would be a Ta(III) species or perhaps comprises oxide and hydride ligands in O═Ta^{2+}−H, which would be an oxidatively saturated Ta(V) species. Our computations indicate that the hydroxide isomer is more stable than the hydride, O═Ta^{2+}−H, isomer by 116 kJ mol^{-1}. The optimized Ta^{2+}−OH and O═Ta^{2+}−H structures are shown in Figure 1. $TaOH^{2+}$ reacted with H_2O by proton transfer to yield

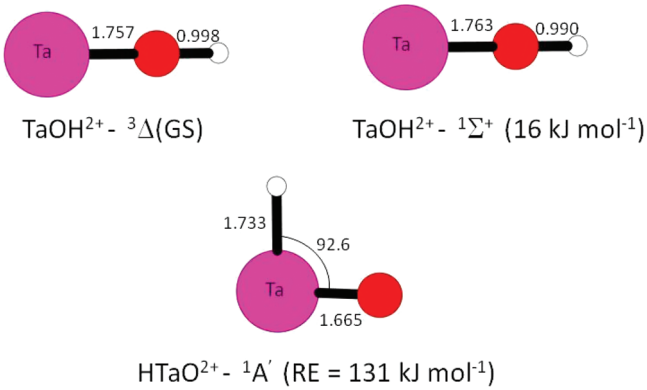

Figure 1. $TaOH^{2+}$ ground-state and two low-energy isomers. The relative energies (RE) are given with respect to the ground-state isomer. Bond lengths are given in angstroms and angles in degrees.

TaO^+ and H_3O^+ with a moderate efficiency (k/k_{COL} = 0.23, k = 1.01 × 10^{-9} cm^3 $molecule^{-1}$ s^{-1}).

Reactions of TaO^{2+} with Oxidants: Formation of TaO_2^{2+}. The reactions of TaO^{2+} with N_2O, H_2O, O_2, CO_2, and CO were studied, and the results are presented in Table 3. Electron transfer to produce TaO^+ prevailed in all cases, but with N_2O, formation of TaO_2^{2+} was observed as a significant (30%) pathway. A mass spectrum illustrating the formation of TaO_2^{2+} as a secondary product in the reaction of Ta^{2+} with N_2O is shown in Figure 2. From reactions of monopositive ions, it was established that the TaO^+ and TaN^+ peaks are from both the Ta^{2+}/N_2O and the Ta^+/N_2O reactions; the $TaNO^+$ product is from the TaN^+/N_2O reaction. TaO_2^+ is due to electron transfer from N_2O to TaO_2^{2+}, a process discussed below, and is also a product of the oxidation of TaO^+ and $TaNO^+$ by N_2O.

Table 3. Reactions of TaO^{2+}[a]

	N_2O	H_2O	O_2	CO_2	CO
TaO^{2+}	0.54 [0.62]	0.28 [1.22]	0.48 [0.54]	0.095 [0.13]	0.099 [0.14]
	TaO_2^{2+}/ 30% TaO^+/70%	TaO^+/ 100%	TaO^+/ 100%	TaO^+/ 100%	TaO^+/ 100%

[a]The reaction efficiencies, k/k_{COL}, are given; the values in brackets are the pseudofirst-order reaction rate constants, k, in units of 10^{-9} cm^3 $molecule^{-1}$ s^{-1}. The absolute values are considered accurate to ±50%; the relative values for comparative purposes are considered accurate to ±20%.

Three plausible structures for TaO_2^{2+} are the dioxide, {O−Ta−O}$^{2+}$, a side-on {Ta−(η^2−O_2)}$^{2+}$ cyclic structure with significant O−O bonding, and an end-on {Ta−(η^1−O_2)}$^{2+}$ structure with a terminal O−O bond. Both neutral TaO_2 and cationic TaO_2^+ have been shown to have bent dioxide structures by spectroscopy and computations.[2,10,12,42] If the TaO_2^{2+} ion is the dioxide, it seems improbable that the metal center would be in a prohibitively high hexavalent oxidation state as in {O═Ta^{VI}═O}$^{2+}$; however, a stable pentavalent tantalum species might be a species with intermediate single/double Ta−O bond character, as represented by the two resonance structures: {O═Ta^{V}−O}$^{2+}$ ↔ {O−Ta^{V}═O}$^{2+}$.

Computational Studies: Geometry and Electronic Structure of TaO_2^{2+} and TaO^{2+}. Geometry optimizations for TaO_2^{2+} were performed considering a number of alternative conformations, including the dioxide structure, as well as the end-on (η^1) and side-on (η^2) O_2-coordination modes. Different initial structures were chosen for each of the considered conformations. Our computations indicate that the TaO_2^{2+} ground state (GS) has a dioxide structure with the C_{2v} point group symmetry and the $^2B_2$ electronic ground state. The TaO_2^{2+} GS structure is shown in Figure 3 together with three low-energy isomers.

NBO, AIM, and ELF analysis were performed on the TaO_2^{2+} GS structure. The partial charge on the metal atom is 3.00 (2.54) according to AIM (NPA) computations. The spin density and, therefore, the unpaired electrons are mainly localized on the oxygen atoms. In particular, the values of the spin density distribution obtained by AIM are 0.33 on the oxygen atoms and −0.15 on the metal.

Transition metal oxides with oxygen-centered radical character are not unusual.[42−44] In a recent theoretical study, Zhao et al. presented a systematic DFT study of the structure and bonding properties of transition metal oxide clusters from groups 3 to 7 (neutral, monopositive, and negative) containing oxygen-centered radical character.[43] In that study, it was predicted that all of the 3d−5d transition metals on the bottom-left side of the V−Mo−Re line are able to form this kind of species. Gas-phase clusters containing the O^- radical species are used as models for transition metal oxide catalysts, which have been shown to exhibit enhanced activity and selectivity for specific reactions due to the presence of radical oxygen atoms. HfO_2^+ and ZrO_2^+ were shown to form oxygen-centered radical structures with geometries similar to the TaO_2^{2+} structure reported here.[43,44]

According to AIM analysis, the Ta−O bond order of the GS TaO_2^{2+} structure is 1.76. This bond order was calculated using the delocalization index, which accounts for the electrons delocalized or shared between the atomic basins, and corresponds to the topological bond order defined by Ángayán

dx.doi.org/10.1021/jp300294c | J. Phys. Chem. A 2012, 116, 3534−3540

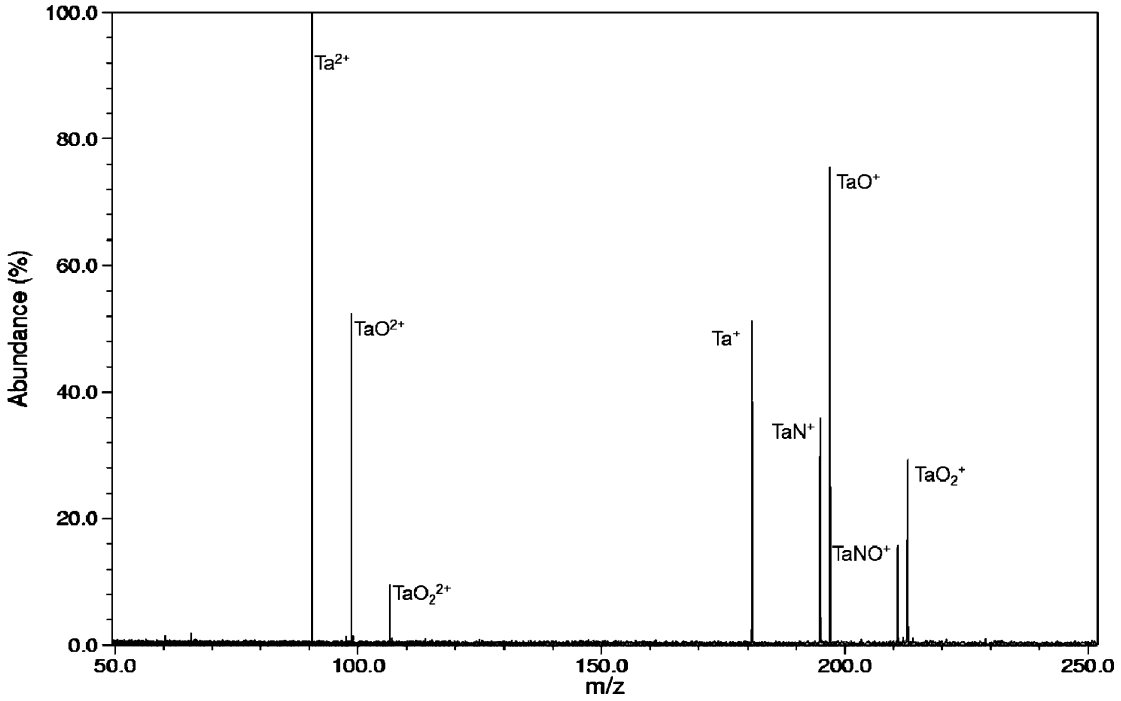

Figure 2. Mass spectrum for the Ta^{2+}/N_2O reaction showing the formation of TaO^{2+} and TaO_2^{2+} (9.8×10^{-8} Torr N_2O; ca. 1×10^{-6} Torr Ar; reaction time 0.5 s).

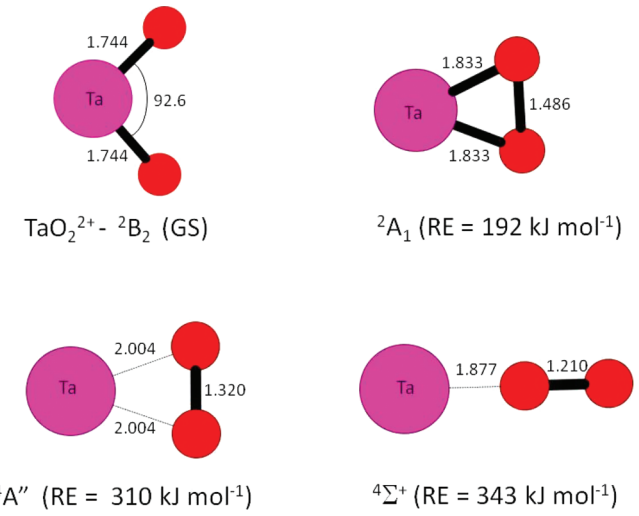

Figure 3. TaO_2^{2+} ground-state and three low-energy isomers. Relative energies (RE) are given with respect to the ground-state isomer. Bond lengths are given in angstroms and angles in degrees.

et al.[45] The (3, −1) Ta−O BCPs (bond critical points) are characterized by a charge density, ρ_{BCP}, of 0.228 au; a Laplacian, $\nabla^2\rho_{BCP}$, of 0.860 au, and an ellipticity, ε, of 0.08 au. ELF analysis indicates that each of the Ta−O bonds is characterized by the presence of two disynaptic valence basins, V(Ta,O), with a total electron population of 3.01 electrons. The contribution to the electron population of the disynaptic valence basins comes mainly from the oxygen atoms (93%), which is an indication of a highly polarized covalent bond. The monosynaptic valence basins, V(O), which in ELF analysis represent the O lone pairs, have a total population of 3.57 electrons on each O atom.

The topological (AIM and ELF) bond analyses, therefore, indicate that the TaO_2^{2+} GS structure is characterized by the presence of highly polarized covalent bonds, which have a partial double bond character, as demonstrated by the population of the disynaptic valence basins, V(Ta,O) = 3.01 electrons, the bond order (1.76), and the ellipticity value (ε = 0.08 au). The picture of the TaO_2^{2+} GS obtained by ELF and AIM analyses is in agreement with the description obtained by NBO, which also indicates the presence of double bonds. The σ-bond is formed from a Ta 91% d−8% s hybrid and a 90% p−10% s O hybrid. The π-bond is formed from the superposition of pure p-oxygen orbitals and pure d-Ta orbitals. The polarization coefficients (e.g., 0.89 for O and 0.45 for Ta) indicate that the Ta−O bond is highly polarized. These results are essentially in accord with the $\{O{=}Ta^{V}{-}O \leftrightarrow O{-}Ta^{V}{=}O\}^{2+}$ resonance picture presented above.

Several low-energy isomers of the TaO_2^{2+} GS structure were identified (Figure 3). An isomer characterized by a cyclic structure with the C_{2v} symmetry and the $^2A_1$ electronic state was found 192 kJ mol^{-1} higher in energy than the GS structure. The O−O distance is typical of peroxides (1.486 Å) and the Ta−O distance is almost 0.1 Å longer than the corresponding value for the dioxide GS structure. A side-on (η^2) O_2 complex in the quartet spin state was found 310 kJ mol^{-1} above the GS structure, which has an O−O bond distance typical of superoxides (1.320 Å). A quartet spin state isomer containing a η^1−O_2 terminal unit and an O−O length very close to that of the free O_2 molecule (1.210 Å) was found 343 kJ mol^{-1} above the GS structure (Figure 3). A η^1−O_2 terminal structure was also identified in the doublet spin state, geometrically and energetically very close to the reported η^1−O_2 quartet spin state isomer. However, the η^1−O_2 doublet spin structure was found to suffer from spin contamination issues; this was the only case in which spin contamination issues were detected.

Our computations indicate that the TaO^{2+} GS has a $^2\Delta$ electronic state, with a Ta−O bond distance of 1.662 Å, which is 0.082 Å shorter than the corresponding value in the TaO_2^{2+} GS dioxide. The partial atomic charge on the metal is 2.63

dx.doi.org/10.1021/jp300294c | J. Phys. Chem. A 2012, 116, 3534−3540

(2.47) according to AIM (NPA) computations. In contrast to the TaO_2^{2+} GS structure, the monoxide shows the unpaired spin density (0.5) entirely localized on the metal atom. The rest of the bonding properties give some indication of the higher strength of the Ta−O bond in the monoxide, in comparison with that of TaO_2^{2+}. In particular, the topological bond order is 2.36, and the charge density at the (3, −1) TaO^{2+} BCP is 0.280 au. ELF analysis indicates that the population of the dysinaptic V(Ta,O) basin is very close to that of TaO_2^{2+} (2.93 electrons).

Reactions of TaO_2^{2+}: Activation of H_2, Oxidation of CO, and Catalytic Oxidation of CO by N_2O. TaO_2^{2+} reacted with N_2O, CO_2, and CO by electron transfer to give TaO_2^{+}, with the kinetics as specified in Table 4. The TaO_2^{2+}/CO_2 and TaO_2^{2+}/CO reactions were studied by isolating Ta^{2+}, pulsing in N_2O to produce TaO_2^{2+}, and allowing isolated TaO_2^{2+} to react with CO_2 or CO present at constant pressure.

Table 4. Reactions of TaO_2^{2+}[a]

	N_2O	CO_2	CO	H_2
TaO_2^{2+}	0.43 [0.60] TaO_2^{+}/100%	0.54 [0.72] TaO_2^{+}/100%	0.52 [0.71] TaO^{2+}/30% TaO_2^{+}/70%	0.11 [0.32] TaO_2H^{2+}/100%

[a]The reaction efficiencies, k/k_{COL}, are given; the values in brackets are the pseudofirst-order reaction rate constants, k, in units of 10^{-9} cm^3 $molecule^{-1}$ s^{-1}. The absolute values are considered accurate to ±50%; the relative values for comparative purposes are considered accurate to ±20%.

TaO_2^{2+} was able to activate H_2 with formation of TaO_2H^{2+}, as also shown in Table 4. The TaO_2^{2+}/H_2 reaction was again studied by isolating TaO_2^{2+} from the reaction of Ta^{2+} and pulsed in N_2O, and allowing it to react with H_2. The TaO_2H^{2+} ion produced in this reaction is presumably the pentavalent oxide hydroxide, $\{O{=}Ta^{V}{-}OH\}^{2+}$; the ability of TaO_2^{2+} to activate H_2 is in accord with the computed oxygen-centered radical character. Recent matrix isolation spectroscopic studies have shown that neutral Ta oxides are also capable of dihydrogen activation.[46,47]

As indicated in Table 4, it was also found that, concomitantly with electron transfer (70% branching ratio), TaO^{2+} was formed in the reaction of TaO_2^{2+} with CO (30% branching ratio), demonstrating the oxidation of CO to CO_2 by TaO_2^{2+}. Combining this reaction with the oxidation of TaO^{2+} to TaO_2^{2+} by N_2O, it becomes evident that the TaO^{2+}/TaO_2^{2+} couple can act as a catalyst in the oxidation of CO by N_2O. This catalytic cycle was verified by exposing Ta^{2+} to a mixture of N_2O and CO: the TaO_2^{2+} product of oxidation by N_2O was isolated; the depletion of the isolated TaO_2^{2+} concomitant with in-growth of TaO^{2+} reveals oxidation of CO to CO_2, demonstrating the oxidation of CO by N_2O mediated by the TaO^{2+}/TaO_2^{2+} couple. The overall catalytic cycle is presented in Figure 4, where the O-transfer processes are indicated in green and the electron-transfer processes, that terminate the cycle by depletion of both TaO^{2+} and TaO_2^{2+}, are indicated in red. The reaction efficiencies for each step of the catalytic cycle are found in Tables 3 and 4. As a result of the relatively high efficiencies of the electron-transfer reactions of TaO^{2+} and TaO_2^{2+} with both N_2O and CO, the overall turnover rate for the catalytic cycle shown in Figure 4 must be low. The thermodynamic requirement for transfer of an O-atom from N_2O to CO via TaO_2^{2+} is 167 kJ mol^{-1} = $D[N_2{-}O] \leq D[OTa^{2+}{-}O] \leq D[OC{-}O]$ = 532 kJ mol^{-1} (see Table 2).

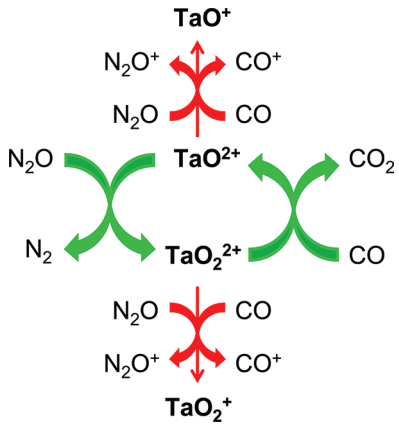

Figure 4. Cycle showing the pair TaO^{2+}/TaO_2^{2+} as catalyst in the oxidation of CO by N_2O (O-transfer processes are indicated in green, and electron-transfer processes, that terminate the cycle by depletion of both TaO^{2+} and TaO_2^{2+}, are indicated in red).

Because $D_0[OTa^{+}{-}O]$ = 587 ± 12 kJ mol^{-1},[2] it is not thermodynamically feasible for TaO_2^{+} to transfer an O atom to CO.

Several examples of metal−ion mediated gas-phase catalytic oxidations, mainly involving N_2O, have been reported in the past decade;[48−53] in the first such demonstration by Kappes and Staley,[54] ca. 30 years ago, the Fe^{+}/FeO^{+} couple was employed for the oxidation of CO by N_2O. We have previously shown that some doubly charged lanthanide and actinide oxides, namely, LaO^{2+}, GdO^{2+}, LuO^{2+}, CmO^{2+}, and PaO_2^{2+}, mediated the catalytic oxidation of CO by N_2O.[18,19]

Electron-Transfer Reactions of Ta^{2+}, TaO^{2+}, and TaO_2^{2+}: Second Ionization Energies of Ta, TaO, and TaO_2. We have previously employed the relative efficiencies of electron transfer from N_2O, CO_2, and CO to doubly charged actinide and lanthanide oxides to provide estimates of the second ionization energies of the corresponding neutrals.[17−19] The method involves the comparison of the electron-transfer efficiencies with those for selected bare M^{2+} ions (M = Sn, Pb, Mn, Ge, and Bi) used for calibration; these efficiencies, reported previously,[17,18] are summarized in Table 5.

Table 5. Electron-Transfer Efficiencies for Dipositive Metal Ions[a]

$M^{2+}/IE[M^{+}]$ (eV)	N_2O	CO_2	CO
$Sn^{2+}/14.63$	0.010	<0.001	<0.001
$Pb^{2+}/15.03$	0.11	0.008	0.002
$Mn^{2+}/15.64$	0.44	0.014	0.017
$Ge^{2+}/15.93$	0.55	0.22	0.027
$Bi^{2+}/16.69$	0.40	0.34	0.24

[a]The electron-transfer efficiencies, k/k_{COL}, are from refs 17 and 18. The $IE[M^{+}]$ are from ref 26.

As indicated in Table 3, TaO^{2+} reacts only by electron transfer with CO_2 and CO; with N_2O both electron transfer and oxidation to TaO_2^{2+} occur (oxidation branching ratio 30%). Referring to Tables 3 and 5, the electron-transfer kinetics for TaO^{2+} with CO_2 suggest that $IE[TaO^{+}]$ lies between $IE[Mn^{+}]$ = 15.64 eV and $IE[Ge^{+}]$ = 15.92 eV, evidently closer to $IE[Ge^{+}]$; the kinetics with CO suggest that $IE[TaO^{+}]$ lies between $IE[Ge^{+}]$ and $IE[Bi^{+}]$ = 16.69 eV. We estimate $IE[TaO^{+}]$ = 16.0 ± 0.5 eV. This estimate is considered

dx.doi.org/10.1021/jp300294c | J. Phys. Chem. A 2012, 116, 3534−3540

particularly uncertain due to the apparent discrepancy between the results with CO_2 and those with CO, as is reflected in the rather large assigned uncertainty of 0.5 eV.

As indicated in Table 4, TaO_2^{2+} reacts only by electron transfer with N_2O and CO_2, while with CO an alternative reaction pathway involving O-atom transfer also occurs (branching ratio 30%). The results indicate that IE[TaO_2^+] is higher than IE[Bi^+] = 16.69 eV. As indicated previously, TaO_2^{2+} reacted with H_2 (IE[H_2] = 15.43 eV[40]) to form TaO_2H^{2+} (k/k_{COL} = 0.11, see Table 4); given the fairly efficient occurrence of H-atom transfer from H_2, it is possible that a minor (i.e., k/k_{COL} < 0.01) electron-transfer channel went undetected. However, TaO_2^{2+} did not exhibit electron-transfer with N_2 (IE[N_2] = 15.58 eV[40]) or Ar (IE[Ar] = 15.76 eV[40]). As it has been established that the minimum difference in ionization energies for electron transfer from a neutral to a dipositive ion is 1−1.5 eV,[17−19,21−23] the absence of electron transfer from N_2 to TaO_2^{2+} suggests an upper limit for IE[TaO_2^+] of {15.58 + 1.5 eV} = 17.1 eV. The results thus bracket IE[TaO_2^+] between 16.69 and 17.1 eV, and we suggest a value of IE[TaO_2^+] = 16.9 ± 0.4 eV, assigning a conservative uncertainty.

The electron-transfer reactions observed in the case of Ta^{2+} with N_2O, CO_2, and CO, indicated in Table 1, allow us to make a new estimate of the second ionization energy of Ta. The existing literature value of IE[Ta^+] = 16.2 ± 0.5 eV is an estimate made by Moore based on spectroscopic data.[41] The observed efficiencies of electron transfer from N_2O, CO_2, and CO to Ta^{2+} are included in Table 1. For N_2O and CO_2, electron transfer is a minor channel such that those kinetics are inconclusive for estimating IE[Ta^+]. The electron-transfer efficiency for Ta^{2+} with CO is between those for Mn^{2+} and Ge^{2+}, lying only slightly below the efficiency for the latter; we conclude that IE[Ta^+] is only slightly lower than IE[Ge^+], and specifically propose IE[Ta^+] = 15.8 ± 0.3 eV. The smaller uncertainty assigned to this value reflects that the efficiency brackets the value between the rather similar IE[Mn^+] and IE[Ge^+], and is particularly close to the latter, and also that this particular evaluation directly compares bare dipositive metal ions. The new value of IE[Ta^+] = 15.8 ± 0.3 eV is lower than Moore's estimate of 16.2 ± 0.5 eV[41] but is within the assigned uncertainty. Our experimental estimate is in good agreement with the estimates of 15.5 eV and 15.85 ± 0.37 eV derived from multiconfiguration Dirac−Fock calculations[55] and artificial neural networks,[56] respectively, providing confidence in the validity of both approaches.

Bond Dissociation Energies of TaO^{2+} and TaO_2^{2+}: Experimental Estimates and Theoretical Calculations. The second ionization energy estimates from the previous section, together with the reliable Ta−O bond dissociation energies of TaO^+ (676 ± 12 kJ mol^{-1}) and TaO_2^+ (587 ± 12 kJ mol^{-1}) recently reported by Armentrout and co-workers,[2] allow us to obtain the following estimates for the bond dissociation energies of doubly charged Ta monoxide and dioxide: $D[Ta^{2+}-O]$ = 657 ± 58 kJ mol^{-1} and $D[OTa^{2+}-O]$ = 500 ± 63 kJ mol^{-1}, based on eqs 1 and 2 below (where the root-sum-of-squares method is employed to arrive at the assigned uncertainties):

$$D[Ta^{2+}-O] = D[Ta^{+}-O] + IE[Ta^{+}] - IE[TaO^{+}] \quad (1)$$

$$D[OTa^{2+}-O] = D[OTa^{+}-O] + IE[TaO^{+}] - IE[TaO_2^{+}] \quad (2)$$

It should be noted that the above estimates are in accord with our experimental observations: $D[Ta^{2+}-O] \geq D[OC-O]$ = 532 kJ mol^{-1}, from the formation of TaO^{2+} in the reaction of Ta^{2+} with CO_2 (see Table 1), and $D[OTa^{2+}-O] \leq D[OC-O]$ = 532 kJ mol^{-1}, from the formation of TaO^{2+} in the reaction of TaO_2^{2+} with CO (see Table 4).

These bond dissociation energies were also computed at the B3LYP/SDD (Ta):TZVP (O) level with the following results: $D_0[Ta^{2+}-O]$ = 637 kJ mol^{-1} and $D_0[OTa^{2+}-O]$ = 389 kJ mol^{-1}. The computed $D_0[Ta^{2+}-O]$ is only 20 kJ mol^{-1} lower than the experimentally derived value, well within the assigned uncertainty. However, the computed $D_0[OTa^{2+}-O]$ is ca. 110 kJ mol^{-1} lower than the experimentally derived value and is outside of the assigned uncertainty range. Assuming that the actual $D_0[OTa^{2+}-O]$ is near the lower end of the experimental range of 437−563 kJ mol^{-1}, we conclude that the computed value is still too low, by ca. 50 kJ mol^{-1}; this deviation is somewhat greater than would generally be expected from this level of theory for a such a small molecule as TaO_2^{2+} and may be related to its peculiar electronic structure.

CONCLUSIONS

Gas-phase reactions of Ta^{2+} ions with several oxidants showed that TaO^{2+} could easily be produced by O-atom abstraction from N_2O, H_2O, O_2, and CO_2. Surprisingly, TaO^{2+} was efficiently oxidized to TaO_2^{2+} by N_2O. DFT calculations were performed on this species and indicated that it is a dioxide ion with oxygen-centered radical character. The pair TaO^{2+}/TaO_2^{2+} was found to catalyze the oxidation of CO by N_2O, although the overall catalytic cycle is rather inefficient due to electron-transfer from N_2O and CO to produce the inert monopositive oxides, TaO^+ and TaO_2^+. It was also found that TaO_2^{2+} was able to activate H_2, with formation of TaO_2H^{2+}. Estimates were made for the second ionization energies of Ta, TaO, and TaO_2, and of the bond dissociation energies of doubly charged Ta monoxide and dioxide. These bond dissociation energies were computed at the B3LYP/SDD (Ta):TZVP (O) level: that for the $Ta^{2+}-O$ dissociation energy is in good agreement with the experimental value, whereas that for $OTa^{2+}-O$ is somewhat below the experimental value.

AUTHOR INFORMATION

Corresponding Author

*E-mail: conceicao.oliveira@ist.utl.pt.

Notes

The authors declare no competing financial interest.

ACKNOWLEDGMENTS

This work was supported by the Fundação para a Ciência e a Tecnologia (projects PTDC/QUI-QUI/108977/2008 and PEst-OE/QUI/UI0100/2011, and Ph.D. grant to M.S.); by the Università della Calabria; and by the U.S. Department of Energy, Office of Basic Energy Sciences, Heavy Element Chemistry program at LBNL under Contract No. DE-AC02-05CH11231 (J.K.G.). This research used resources of the National Energy Research Scientific Computing Center (NERSC), which is supported by the Office of Science of the U.S. Department of Energy under Contract No. DE-AC02-05CH11231.

REFERENCES

(1) Hinton, C. S.; Li, F.; Armentrout, P. B. *Int. J. Mass Spectrom.* **2009**, *280*, 226−234.
(2) Hinton, C. S.; Citir, M.; Manard, M.; Armentrout, P. B. *Int. J. Mass Spectrom.* **2011**, *308*, 265−274.
(3) Ranasinghe, Y. A.; MacMahon, T. J.; Freiser, B. S. *J. Phys. Chem.* **1991**, *95*, 7721−7726.
(4) Parke, L. G.; Hinton, C. S.; Armentrout, P. B. *J. Phys. Chem. A* **2008**, *112*, 10469−10480.
(5) Koyanagi, G. K.; Caraiman, D.; Blagojevic, V.; Bohme, D. K. *J. Phys. Chem. A* **2002**, *106*, 4581−4590.
(6) Lavrov, V. V.; Blagojevic, V.; Koyanagi, G. K.; Bohme, D. K. *J. Phys. Chem. A* **2004**, *108*, 5610−5624.
(7) Blagojevic, V.; Flaim, E.; Jarvis, M. J. V.; Koyanagi, G. K.; Bohme, D. K. *J. Phys. Chem. A* **2005**, *109*, 11224−11235.
(8) Koyanagi, G. K.; Bohme, D. K. *J. Phys. Chem. A* **2006**, *110*, 1232−1241.
(9) Cheng, P.; Koyanagi, G. K.; Bohme, D. K. *J. Phys. Chem. A* **2007**, *111*, 8561−8573.
(10) Zhou, M. F.; Andrews, L. *J. Phys. Chem. A* **1998**, *102*, 8251−8260.
(11) Zhou, M. F.; Andrews, L. *J. Phys. Chem. A* **1998**, *102*, 10025−10031.
(12) Chen, M. H.; Wang, X.; Zhang, L. N.; Yu, M.; Qin, Q. Z. *Chem. Phys.* **1999**, *242*, 81−90.
(13) Zhao, Y. Y.; Zheng, X. M.; Zhou, M. F. *Chem. Phys.* **2008**, *351*, 13−18.
(14) Zhou, M. F.; Zhuang, J.; Wang, G. J.; Chen, M. H. *J. Phys. Chem. A* **2011**, *115*, 2238−2246.
(15) Wang, G. J.; Zhuang, J.; Chen, M. H. *J. Phys. Chem. A* **2011**, *115*, 8623−8629.
(16) Cornehl, H. H.; Heinemann, C.; Marçalo, J.; Pires de Matos, A.; Schwarz, H. *Angew. Chem., Int. Ed.* **1996**, *35*, 891−894.
(17) Gibson, J. K.; Haire, R. G.; Santos, M.; Marçalo, J.; Pires de Matos, A. *J. Phys. Chem. A* **2005**, *109*, 2768−2781.
(18) Santos, M.; Pires de Matos, A.; Marçalo, J.; Gibson, J. K.; Haire, R. G.; Tyagi, R.; Pitzer, R. M. *J. Phys. Chem. A* **2006**, *110*, 5751−5759.
(19) Gibson, J. K.; Haire, R. G.; Santos, M.; Pires de Matos, A.; Marçalo, J. *J. Phys. Chem. A* **2008**, *112*, 11373−11381.
(20) Marçalo, J.; Leal, J. P.; Pires de Matos, A.; Marshall, A. G. *Organometallics* **1997**, *16*, 4581−4588.
(21) Marçalo, J.; Santos, M.; Pires de Matos, A.; Gibson, J. K.; Haire, R. G. *J. Phys. Chem. A* **2008**, *112*, 12647−12656.
(22) Santo, E.; Di; Santos, M.; Michelini, M. C.; Marçalo, J.; Russo, N.; Gibson, J. K. *J. Am. Chem. Soc.* **2011**, *133*, 1955−1970.
(23) Marçalo, J.; Santos, M.; Gibson, J. K. *Phys. Chem. Chem. Phys.* **2011**, *13*, 18322−18322.
(24) Guan, S.; Marshall, A. G. *Int. J. Mass Spectrom. Ion Proc.* **1996**, *157/158*, 5−37.
(25) Su, T.; Chesnavich, W. J. *J. Chem. Phys.* **1982**, *76*, 5183−5185.
(26) Lide, D. R., Ed. *CRC Handbook of Chemistry and Physics*, 88th ed.; CRC Press: Boca Raton, FL, 2007.
(27) Becke, A. D. *J. Chem. Phys.* **1993**, *98*, 5648−5652.
(28) Lee, C. T.; Yang, W. T.; Parr, R. G. *Phys. Rev. B* **1988**, *37*, 785−789.
(29) Pseudopotentials, ECPs. http://www.theochem.unistuttgart.de/pseudopotentiale/.
(30) Kuchle, W.; Dolg, M.; Stoll, H.; Preuss, H. *J. Chem. Phys.* **1994**, *100*, 7535−7542.
(31) Godbout, D.; Salahub, R.; Andzelm, J.; Wimmer, E. *Can. J. Chem.* **1992**, *70*, 560−571.
(32) Frisch, M. J.; Trucks, G. W.; Schlegel, H. B.; Scuseria, G. E.; Robb, M. A.; Cheeseman, J. R.; Scalmani, G.; Barone, V.; Mennucci, B.; Petersson, G. A.; Nakatsuji, H.; Caricato, M.; Li, X.; Hratchian, H. P.; Izmaylov, A. F.; Bloino, J.; Zheng, G.; Sonnenberg, J. L.; Hada, M.; Ehara, M.; Toyota, K.; Fukuda, R.; Hasegawa, J.; Ishida, M.; Nakajima, T.; Honda, Y.; Kitao, O.; Nakai, H.; Vreven, T.; Montgomery, J. A., Jr.; Peralta, J. E.; Ogliaro, F.; Bearpark, M.; Heyd, J. J.; Brothers, E.; Kudin, K. N.; Staroverov, V. N.; Kobayashi, R.; Normand, J.; Raghavachari, K.; Rendell, A.; Burant, J. C.; Iyengar, S. S.; Tomasi, J.; Cossi, M.; Rega, N.; Millam, J. M.; Klene, M.; Knox, J. E.; Cross, J. B.; Bakken, V.; Adamo, C.; Jaramillo, J.; Gomperts, R.; Stratmann, R. E.; Yazyev, O.; Austin, A. J.; Cammi, R.; Pomelli, C.; Ochterski, J. W.; Martin, R. L.; Morokuma, K.; Zakrzewski, V. G.; Voth, G. A.; Salvador, P.; Dannenberg, J. J.; Dapprich, S.; Daniels, A. D.; Farkas, O.; Foresman, J. B.; Ortiz, J. V.; Cioslowski, J.; Fox, D. J. *Gaussian 09*, revision B.01; Gaussian, Inc.: Wallingford, CT, 2009.
(33) Glendening, E. D.; Reed, A. E.; Carpenter, J. E.; Weinhold, F. *NBO*, version 3.1; Gaussian, Inc.: Wallingford, CT, 2009
(34) Bader, R. F. W. *Atoms in Molecules: A Quantum Theory*; Oxford University Press: Oxford, U.K., 1994.
(35) Becke, A. D.; Edgecombe, K. E. *J. Chem. Phys.* **1990**, *92*, 5397−5403.
(36) Silvi, B.; Savin, A. *Nature* **1994**, 683−686.
(37) Noury, S.; Krokidis, X.; Fuster, F.; Silvi, B. *TopMod Package*; Université Pierre et Marie Curie, Paris, 1997.
(38) Noury, S.; Krokidis, X.; Fuster, F.; Silvi, B. *Comput. Chem.* **1999**, *23*, 597−604.
(39) Keith, T. A. *AIMAll*, version 10.12.08; 2010 (see aim.tkgristmill.com).
(40) Linstrom, P. J.; Mallard, W. G.; Eds. *NIST Chemistry WebBook, NIST Standard Reference Database Number 69*; National Institute of Standards and Technology: Gaithersburg, MD, 2011 (see http://webbook.nist.gov).
(41) Moore, C. E. *Atomic Energy Levels as Derived from the Analysis of Optical Spectra*; National Bureau of Standards: Washington, DC, 1958; Vol. *III*.
(42) Wu, Z. J.; Kawazoe, Y.; Meng, J. *J. Mol. Struct.* **2006**, *764*, 123−132.
(43) Zhao, Y.-X.; Ding, X.-L.; Ma, Y.-P.; Wang, Z.-C.; He, S.-G. *Theor. Chem. Acc.* **2010**, *127*, 449−465.
(44) Johnson, G. E.; Mitrić, R.; Tyo, E. C.; Bonačić-Koutecky, V.; Castleman, A. W. Jr. *J. Am. Chem. Soc.* **2008**, *130*, 13912−13920.
(45) Ángayán, J. G.; Loos, M.; Mayer, I. *J. Phys. Chem.* **1994**, *98*, 5244−5248.
(46) Zhou, M. F.; Wang, C. X.; Li, Z. H.; Zhuang, J.; Zhao, Y. Y.; Zheng, X. M.; Fan, K. N. *Angew. Chem., Int. Ed.* **2010**, *49*, 7757−7761.
(47) Zhou, M. F.; Wang, C. X.; Zhuang, J.; Zhao, Y. Y.; Zheng, X. M. *J. Phys. Chem. A* **2011**, *115*, 39−46.
(48) Blagojevic, V.; Jarvis, M. J. Y.; Flaim, E.; Koyanagi, G. K.; Lavrov, V. V.; Bohme, D. K. *Angew. Chem., Int. Ed.* **2003**, *42*, 4923−4927.
(49) Bohme, D. K.; Schwarz, H. *Angew. Chem., Int. Ed.* **2005**, *44*, 2336−2354.
(50) Blagojevic, V.; Orlova, G.; Bohme, D. K. *J. Am. Chem. Soc.* **2005**, *127*, 3545−3555.
(51) Dasic, A.; Zhao, X.; Bohme, D. K. *Int. J. Mass Spectrom.* **2006**, *254*, 155−162.
(52) Blagojevic, V.; Bozovic, A.; Orlova, G.; Bohme, D. K. *J. Phys. Chem. A* **2008**, *112*, 10141−10146.
(53) Bozovic, A.; Feil, S.; Koyanagi, G. K.; Viggiano, A. A.; Zhang, X. H.; Schlangen, M.; Schwarz, H.; Bohme, D. K. *Chem.—Eur. J.* **2010**, *16*, 11605−11610.
(54) Kappes, M. M.; Staley, R. H. *J. Am. Chem. Soc.* **1981**, *103*, 1286−1287.
(55) Fricke, B.; Johnson, E.; Rivera, G. M. *Radiochim. Acta* **1993**, *62*, 15−25.
(56) Sigman, M. E.; Rives, S. S. *J. Chem. Inf. Comput. Sci.* **1994**, *34*, 617−620.